

## Observational Evaluation of the Snow Breeze

M. SEGAL<sup>†</sup>, J. H. CRAMER<sup>†‡</sup>, R. A. PIELKE<sup>†</sup>, J. R. GARRATT<sup>\*\*</sup>, AND P. HILDEBRAND<sup>\*</sup>

<sup>\*</sup>*Department of Physics and Astronomy, University of Kansas, Lawrence, Kansas*

<sup>†</sup>*Department of Atmospheric Science, Colorado State University, Fort Collins, Colorado*

<sup>‡</sup>*Current affiliation: AFGWC/SDDC, Offutt Air Force Base, Nebraska*

<sup>\*\*</sup>*CSIRO, Division of Atmospheric Research, Mordialloc, Victoria, Australia*

<sup>\*</sup>*National Center for Atmospheric Research, Boulder, Colorado*

(Manuscript received 3 April 1990, in final form 31 August 1990)

### ABSTRACT

An observational evaluation of the daytime thermally induced flow between the snow and snow-free areas (termed snow breeze) has been carried out. Aircraft measurements within the lower atmosphere made in the winter of 1988 reveal large temperature reductions over the snow cover relative to the bare ground implying the potential for snow-breeze generation. The aircraft flights were generally made under unfavorable synoptic conditions although in one particular case with a moderate synoptic flow, a snow breeze was clearly identified. A less distinctive snow breeze was indicated in a second case. Observed features and a scaling analysis of relevance to snow breezes are presented.

### 1. Introduction

There has been little systematic observational evaluation of the impact of snow cover on daytime mesoscale flows; in particular, that due to surface thermal forcing when the snow cover lies adjacent to bare ground. In the context of this study we refer to the generation of the "snow breeze" (the term "snow breeze" was introduced in Johnson et al. 1984) across the boundary separating snow-covered and snow-free areas. Noticeable snow-breeze situations are most likely to occur following heavy winter snow storms in relatively southern midlatitudes of the Northern Hemisphere, or in the higher midlatitudes during fall and at the end of winter/early spring (see Segal et al. 1991). However, the often irregular mesoscale spatial distribution of snow cover over uniform terrain, as well as the random nature of its location, make it virtually impossible to evaluate any anticipated snow breeze through the routine synoptic meteorological network.

Evidence is available, through limited documented observations, that daytime meteorological shelter temperatures are noticeably lower over a snow-covered area compared to those above adjacent bare ground under similar environmental conditions (Wash et al. 1981; Bluestein 1982; Schlatter et al. 1983; Johnson et al. 1984). These observations are consistent with the conditions necessary for the generation of the snow breeze.

\* The National Center for Atmospheric Research is supported by the National Science Foundation.

Corresponding author address: Mr. Moti Segal, Dept. of Physics and Astronomy, University of Kansas, Lawrence, KS 66045.

Although no systematic observational study has focused on the effects of snow cover on the generation of the snow breeze and the related modification of the daytime atmospheric boundary layer (ABL), two of the studies mentioned above provide some insight into this problem. Johnson et al. (1984), based on a few surface observations, documented and discussed a weather event involving the possible generation of a snow breeze between bare ground areas and an adjacent snow area. Wash et al. (1981) contrasted surface-layer conditions across the boundary of a rapidly melting snowband on the morning of 15 April 1980 near Cedar Rapids, Iowa (CID); 10 cm of snow depth was reported near the western edge of a mesoscale snowband, but by the end of the day the snow at CID had completely melted. In contrast, Waterloo, Iowa (ALO), located about 90 km to the northwest in the snow-free region, reported no snow cover. Surface weather for the two locations was compared in Fig. 5 of Wash et al. (1981), who attributed the daytime reduction in wind speed at CID to the reduced mixed-layer depth over snow. However, an alternative explanation allows for an induced snow-breeze flow to oppose the generally westerly synoptic flow near the snow boundary, resulting in reduced wind speeds. Their results suggest that a synoptic flow in excess of  $10 \text{ m s}^{-1}$  is strong enough to prevent the development of an opposing snow breeze, although not strong enough to mask the snow-cover effect on the ABL structure and on the snow-cover perturbation to the large-scale flow.

Undoubtedly, additional observational studies are required to evaluate, in detail, the effects of snow cover

on the generation of snow breezes. As such, the present study provides a contribution in this direction through aircraft measurements. In section 2 of this paper, detailed description and interpretation of results from an aircraft field experiment are presented. Scaling and conceptual considerations relating to the circulation intensity observed in the study are given in section 3.

## 2. Aircraft observations across snow-bare ground boundaries

The random location of snow-bare ground boundaries in a given region and their temporal modifications make aircraft the best practical platform to observe the structure of the snow breeze. In addition, the short time response of the aircraft allows for efficient operations, with observations focused on those days with more favorable synoptic conditions. In order to utilize this observational tool, a project entitled Snow Shading Boundary-Layer Interaction Measurements (SSBLIM) was carried out during the period 1 February–19 March 1988. A detailed description of the SSBLIM experiment and its main results are given in Cramer (1988).

### a. Aircraft instrumentation and flight procedures

The aircraft used in the SSBLIM project was the NCAR King Air N312D. It was instrumented so that aircraft position and height, wind velocity, air temperature, IR surface temperature, and surface albedo could be directly measured or could be derived from measured quantities. The raw data were digitally recorded on magnetic tape (which were later processed) either at a rate of 50 samples per second (sps) or at a 5-sps frequency depending on the instrument. During the processing, 50-sps data were filtered at 10 sps and interpolated to 20 sps, and 5-sps data were output to tape as 1-s averages. The sensible heat fluxes were calculated from 20-sps data using eddy correlation techniques (see Cramer 1988). This calibrated and edited final product forms the basis of the dataset used in the present data analysis. Details of the aircraft instrument systems and the data processing procedures can be found in Miller and Friesen (1987), and Lenschow and Spyers-Duran (1987). In addition to the instruments mentioned above, forward- and downward-looking video cameras with recorders and date/time recordings were mounted on the aircraft.

Each flight pattern of maximum duration  $\sim 4\text{--}5$  h and aircraft speed  $\sim 80\text{ m s}^{-1}$  consisted of several legs or transects at several altitudes, together with vertical profiles measured about 10–30 km from the snow-bare ground boundary. Generally, transects (each at a constant altitude) were flown after the first vertical “sounding” and then repeated about an hour later after the second sounding. This repetition provides data allowing atmospheric changes in time to be deduced.

Although the GOES satellite imagery on the NOAA

SERS and the VDOC workstations at Colorado State University (CSU) enabled a relatively accurate appraisal of locations of surface discontinuities, the final location and flight planning were decided in the air. Optimum project weather conditions required a well-defined boundary that was located within aircraft flight range, together with clear skies and light synoptic wind flow. Nine flights were carried out during the SSBLIM experiment. The remainder of this section is devoted to case study descriptions based on the results of three of the SSBLIM flights (denoted by Flight No. 1, No. 2, and No. 3; these flights were the most informative given the objective of the study). The results focus on those parameters which support the generation of snow breezes.

### b. Flight No. 1 (southern Colorado, 12 February 1988)

#### 1) SITUATION

During the period 10–11 February 1988, an arctic air mass surged southeastward down the eastern side of the Rocky Mountains. The system produced significant upslope flow, with snowfall along the eastern Rockies as far south as the Arkansas River Valley in southeast Colorado. As is commonly the case, the storm produced unevenly distributed snow upon the differently oriented slopes.

By the early morning of 12 February the high pressure system had moved to the Gulf Coast regions of Texas and Louisiana (see Fig. 1). The arctic air mass had propagated eastward and Colorado came under

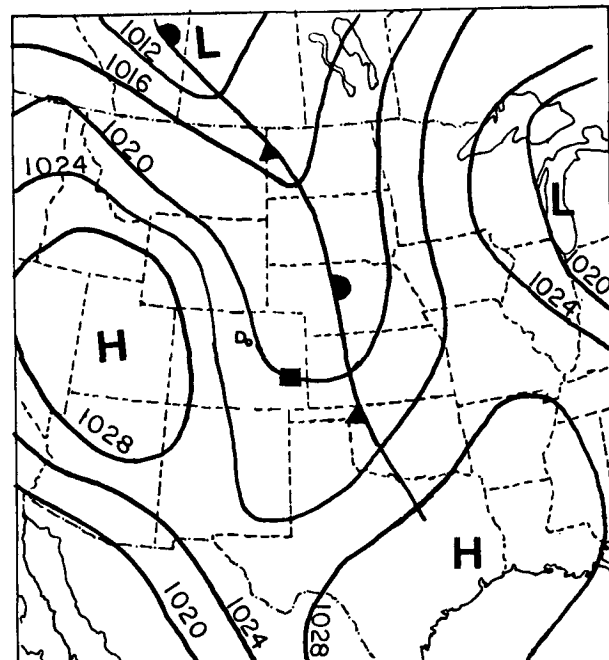


FIG. 1. Surface synoptic weather analysis for 0500 MST 12 February 1988. The location of the flight measurements is shaded. (Reproduced from *Daily Weather Maps*, Climate Analysis Center.)

the influence of a lee trough located over the High Plains. In this case, the south-facing slope north of the Arkansas River was left largely snow covered; the north-facing slope south of the river was left bare. The system thus produced a fairly pronounced north–south discontinuity in snow cover just north of the Arkansas River near La Junta (LHX) (Fig. 2a). (Note that the locations and station names on all presented satellite imageries are part of the NWS synoptic network). The planned flight pattern was positioned over the snow boundary near LHX as shown by the alternate light–dark line in Fig. 2a.

## 2) MEASUREMENTS

By early afternoon a distinct surface temperature gradient had developed across the snow boundary, as indicated by the GOES IR temperature imagery (see Figs. 2b,c). The relatively sharp transition from bare ground to snow cover is evidenced by a decrease of  $\sim 7$  K in the surface temperature over  $\sim 10$ -km distance. An even greater temperature gradient existed about 20 km west of the chosen transect ( $\sim 1$  K  $\text{km}^{-1}$ ).

It should be noted that the resolution of IR temperature data was  $4 \text{ km} \times 8 \text{ km}$  (pixel size), so that some spatial smoothing of the temperature change at the boundary occurs. As will be seen later, the actual temperature change over a 10-km distance near the snow boundary (as measured by the aircraft) was about twice that observed by the satellite. The relative change in the terrain elevation along the flight transect is shown in Fig. 3a, indicating a relatively small slope along the snow-covered portion of the transect (see Fig. 2a for the flight transect location and orientation). Figure 3b illustrates the significant change in albedo that occurred from the bare ground to the snow cover, coincident with a relatively large change in surface temperature from 290 K to 273 K (Fig. 3c). Note that the albedo and the surface temperature data indicate that snow cover was mainly uniform for a distance of about 20 km from the boundary and patchy beyond. The sharp, narrow region of surface temperature fall to near 273 K at about the 17-km location represents the aircraft's crossing of the frozen Arkansas River. It is suggested that for this case, the combined effect of a snow breeze and a thermally induced slope flow should occur.

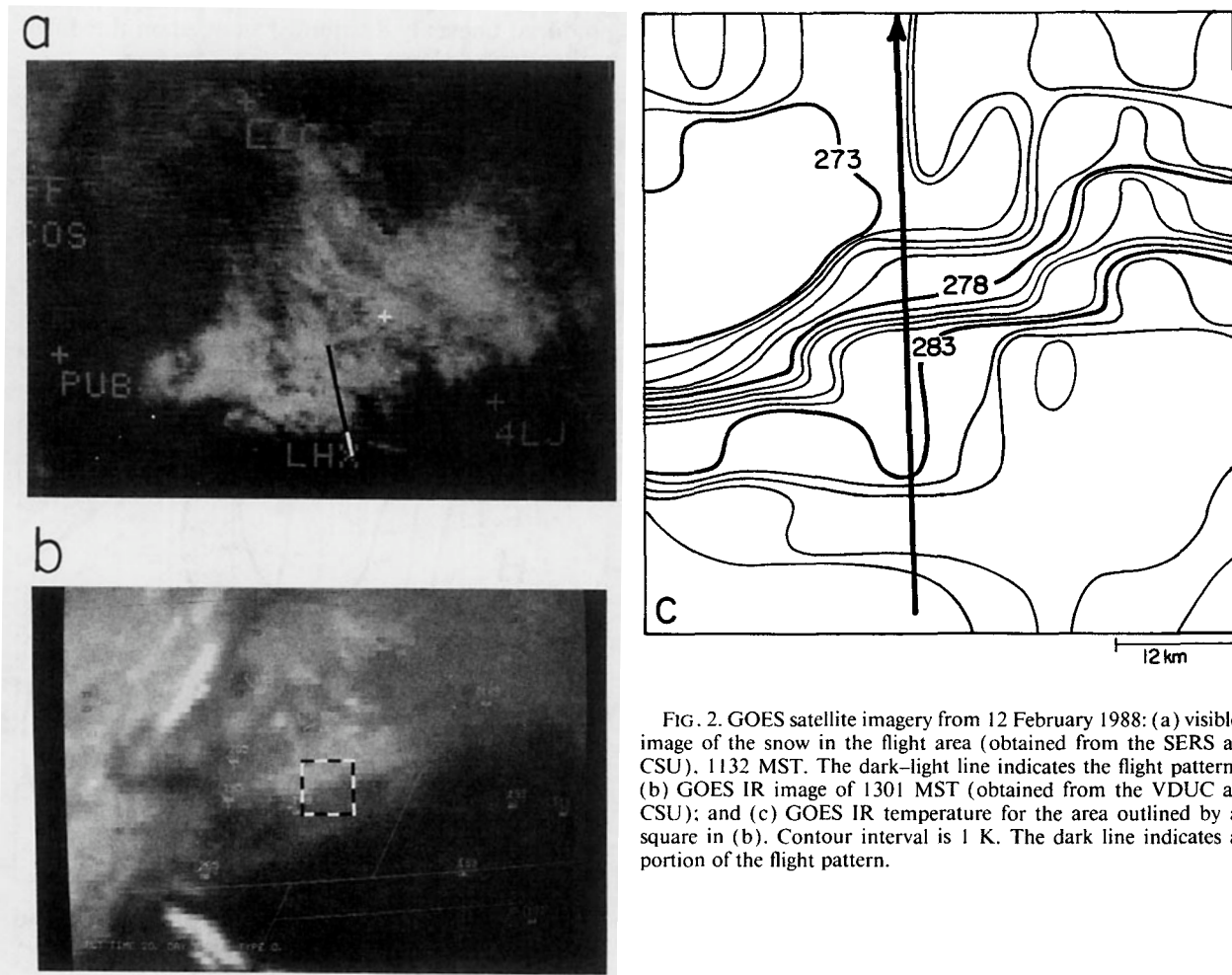


FIG. 2. GOES satellite imagery from 12 February 1988: (a) visible image of the snow in the flight area (obtained from the SERS at CSU), 1132 MST. The dark–light line indicates the flight pattern; (b) GOES IR image of 1301 MST (obtained from the VDUC at CSU); and (c) GOES IR temperature for the area outlined by a square in (b). Contour interval is 1 K. The dark line indicates a portion of the flight pattern.

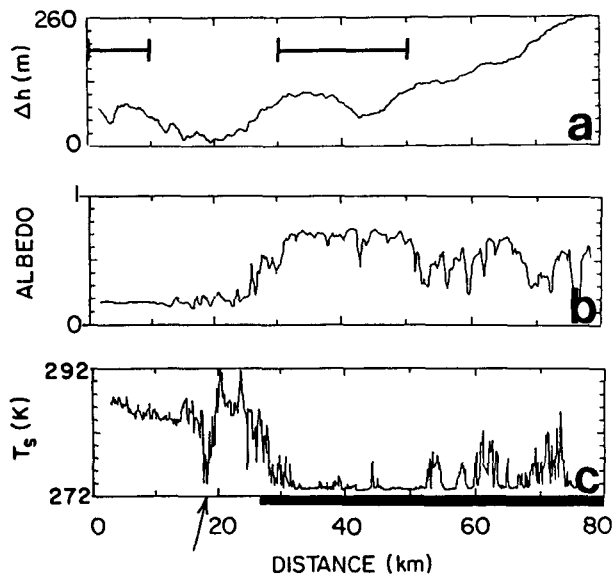


FIG. 3. Aircraft observations of: (a) terrain elevation relative change,  $\Delta h$ ; the horizontal bars indicate the locations of the vertical profile measurements presented later; (b) surface albedo; and (c) surface temperature,  $T_s$ , for Flight No. 1 based on flight altitude data measured at 95 m from 1248:48–1313:24 MST. The dark line indicates the snow-covered portion of the transect. The arrow indicates the location of the frozen Arkansas River. See Figs. 2a,b for flight transect.

Figure 4 presents soundings at two sites, located about 50 km apart, over the snow and the snow-free ground (the bars in Fig. 3a indicate their locations). The vertical profiles of  $\theta$  (Figs. 4a,b) show that a convectively mixed layer had developed over the snow-free region to a height of over 1000 m. The lower atmosphere over the snow, on the other hand, was strongly stable. In the lowest 200 m above the snow cover,  $\theta$  increased by  $\sim 5$  K; above this layer the stratification is slightly stable. Both vertical profiles of  $\theta$  are for similar terrain altitude and are therefore closely comparable. The difference in the thermal stratification is attributed to suppression of the surface sensible heat flux over the snow and to advection by the background flow of relatively warm air over the snow surface. Differences in the wind direction and speed over the two regions are also illustrated in the profiles (Figs. 4c–f). The background flow for this case was quite complicated, with an interaction of the synoptic flow and the thermally forced upslope flow. The resultant wind, as is seen above 100 m in the vertical profiles, was generally southerly at  $5\text{--}9\text{ m s}^{-1}$ , with the flow over the snow (above 100 m) being slightly more westerly in direction and significantly stronger in speed. This flow should be a closer approximation to the synoptic flow than the flow observed over the bare ground region,

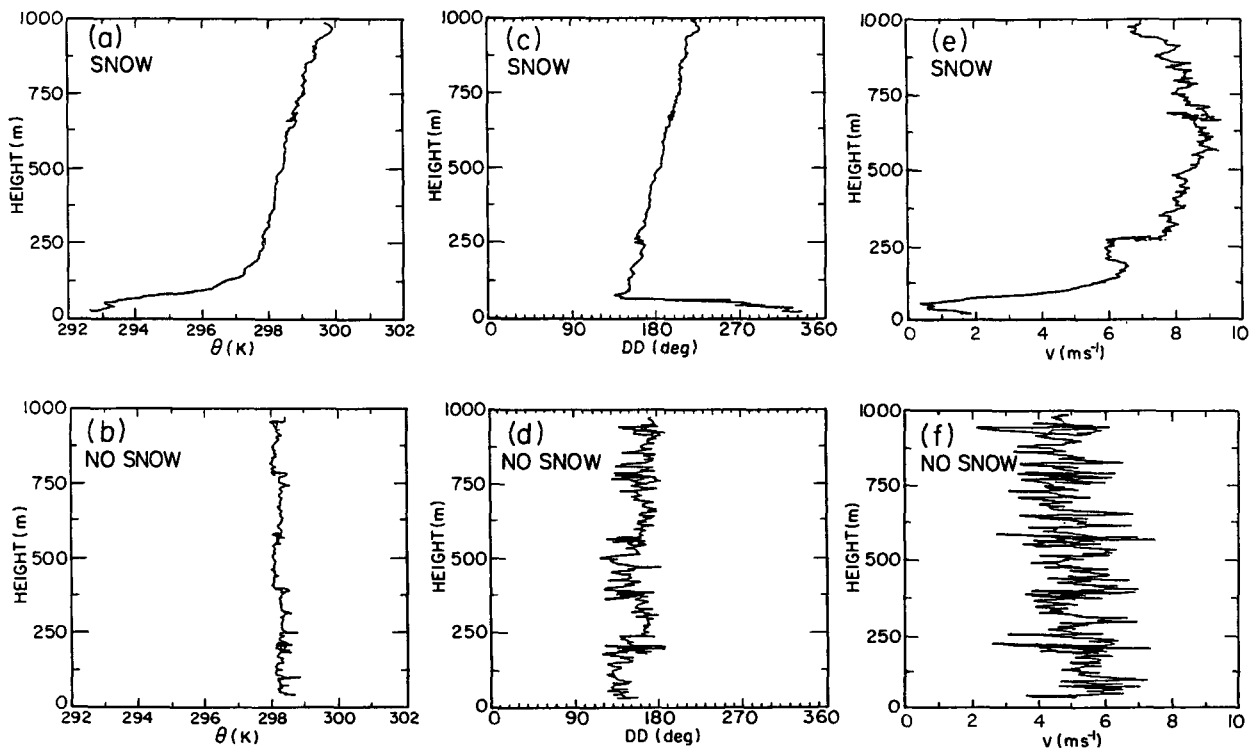


FIG. 4. Vertical profiles of several variables from Flight No. 1 at the locations indicated on Fig. 3a. Measurements over the snow-free ground were made from 1230:00–1257:10 MST; measurements over the snow were made from 1416:55–1435:00 MST. (a–b) Potential temperature,  $\theta$ ; (c–d) wind direction,  $DD$ ; and (e–f) wind speed,  $V$ .

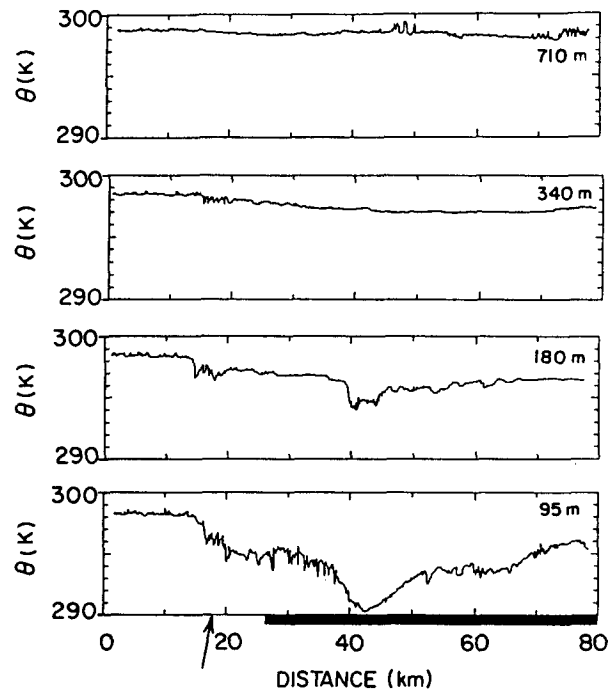


FIG. 5. Cross section of the potential temperature,  $\theta$ , for Flight No. 1 at various altitudes (leg 95 m from 1248:48–1313:24 MST; 180-m data measured from 1316:20–1332:00 MST; 340-m data measured from 1334:18–1348:30 MST; 710-m data measured from 1352:10–1408:00 MST). The dark line indicates the snow-covered portion of transect.

since there is both a smaller frictional effect and an expected smaller upslope thermal forcing over the snow. More significant differences in the winds between the two regions were found in the layer below 100 m. In this layer the flow over the snow-free region was southerly at  $4\text{--}5\text{ m s}^{-1}$  compared with a north-northwesterly wind at nearly  $2\text{ m s}^{-1}$  over the snow (note that differences in the speed profiles should be attributed, in part, to differences in the vertical mixing between the snow and the snow-free sections). As will be seen in the data from the horizontal legs, this north-northwesterly opposing wind can be identified as a snow breeze. Finally, it is worth noting the significant turbulence seen in the wind profiles over the snow-free ground.

Data from the horizontal transects flown across the snow boundary at heights of 95, 180, 340, and 710 m AGL for the potential temperature, wind direction, and wind speed are presented in Figs. 5 and 6, respectively (note that the flight passes were carried out over a period of  $\sim 1\text{ h}$ ). It appears that the presence of the relatively narrow, frozen Arkansas River (at about 17 km along the transects) and the snow region (indicated in the figures) were responsible for several boundary-layer modifications. The most significant horizontal variations in  $\theta$  were found at the lowest flight level of 95 m with significant changes up to a height of 340 m. Values of  $\theta$  decreased as air was advected over the frozen Arkansas River (referring to the figures, air was generally

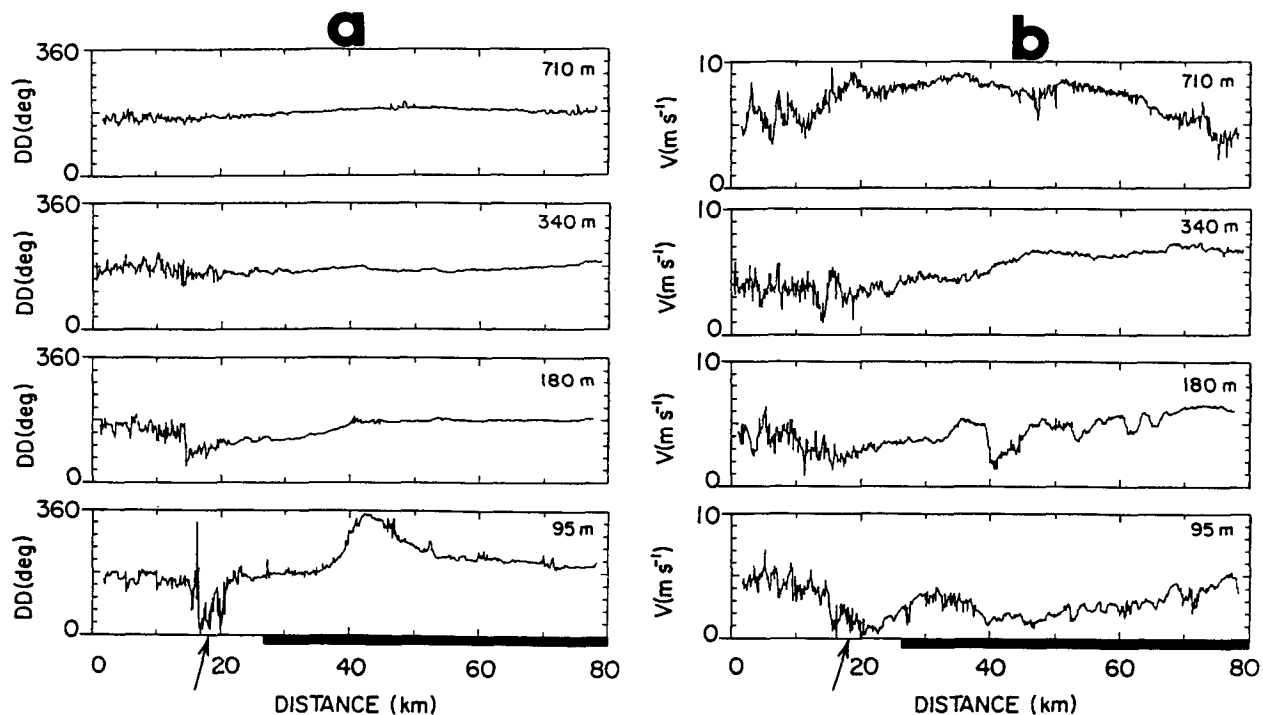


FIG. 6. The same as Fig. 5, except for (a) wind direction,  $DD$ ; and (b) wind speed,  $V$ .

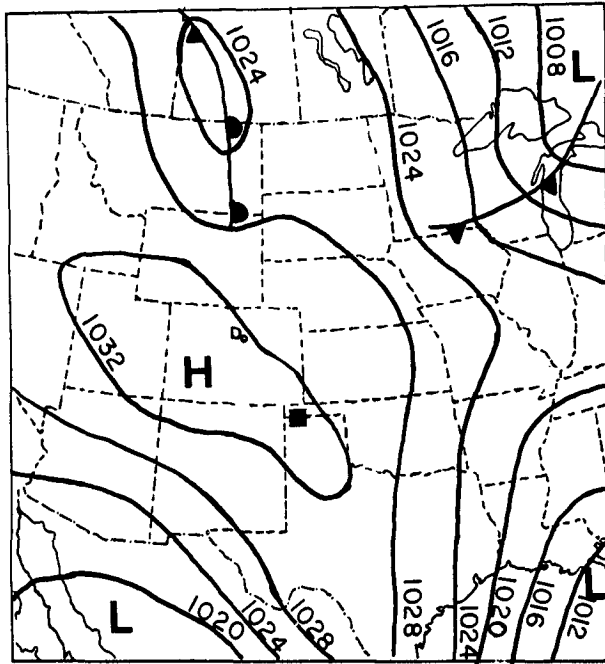


FIG. 7. As Fig. 1, except for 18 March 1988.

being advected by the background flow from the bare soil area toward the snow). The decrease in  $\theta$  from the warmer, bare ground region to the coolest air over the snow was about 8 K at 95 m. Decreases in potential temperature of  $\sim 4.5^\circ\text{K}$  at 180 m and  $\sim 1.5$  K at 340 m were also observed. Similar characteristics of temperature structure in the case of sea breezes associated with offshore background flows were simulated by Mahrer and Segal (1979) and Garratt and Ryan (1989).

Figures 6a,b reveal two zones of wind variations at 95 m, associated with sharp changes in  $\theta$ . Just downwind of the Arkansas River there was a small zone (about 4 km long) with an associated significant wind shift. Instead of the typical southerly background flow of about  $5 \text{ m s}^{-1}$ , this small region had a wind flow of  $1\text{--}2 \text{ m s}^{-1}$  out of the northeast, generally opposing the background flow. As the aircraft proceeded north of the river, the general background flow returned and on reaching the zone of cool air over the snow, another wind shift was detected. In this zone, an apparent snow breeze, which almost directly opposed the background flow, existed. The opposing flow reached a maximum intensity of about  $2 \text{ m s}^{-1}$ . Similar but less significant wind changes occurred at 180 m. Above that height, only differences in the turbulent character of the wind over the two surfaces are evident.

In conclusion, the contrast in the thermal stratification between the snow-covered and snow-free areas implies the development of a snow breeze. The slightly sloped terrain along the snow-covered area, and the

thermally stable ABL there, suggest a contribution from drainage flow components.

### c. Flight No. 2 (Texas Panhandle, 18 March 1988)

#### 1) SITUATION

From 16–18 March 1988 a late winter storm moved southeastward from the Four Corners region into the northern Gulf of Mexico, leaving a snowband stretching from the central Texas Panhandle through northwest Oklahoma and into southeastern Kansas. On the morning of 18 March, the snowband region was under the influence of high pressure centered in western Colorado, with a northwesterly surface geostrophic wind prevailing across the region (see Fig. 7).

As seen in the satellite imagery (see Fig. 8a), fairly sharp snow–bare ground boundaries existed along the northwest and southeast sides of the snowband. The band was fresh, relatively deep [a maximum snow depth of 30 cm was reported at Gage, Oklahoma (GAG)], had sharp boundaries, and existed over only slightly inclined terrain. The chosen flight location and orientation are shown in Fig. 8a, with the snow-covered region for this flight being patchy and melting, with areas of bare ground clearly visible.

#### 2) MEASUREMENTS

The surface temperature gradients across the surface discontinuity were significant and relatively large by early afternoon (Figs. 8b,c). Across the snow boundary near the chosen flight location, a surface temperature change of 8 K in 11 km was observed by satellite ( $\sim 0.7 \text{ K km}^{-1}$ ). The albedo and surface temperature variation (based on the 90-m flight transect) indicated a significant contrast between the bare ground and the patchy snow (Figs. 9b,c; see Fig. 8 for flight transect location and orientation) with the surface temperature difference being roughly 18 K across the transect (from about 297 K over the bare ground to about 279 K over the patchy snow). The snow surface temperature is higher than that measured in Flight No. 1 indicating less uniform snow cover, as supported by measured albedo in both flights.

Figure 10 provides an illustration of the daily shelter temperature contrast between the snow free locations 1K5 and AMA, compared with GAG, which is snow covered (see Fig. 8a for site locations). The temperature difference during the afternoon hours reached values as high as 10 K. Comparisons of such values with summertime shelter temperature differences between near-shore and inland locations (in association with sea breezes) are given in section 3.

The vertical profile measurements revealed very different boundary-layer structure over the snow-covered and snow-free regions (Fig. 11). However, since the two profiles were measured about 1.5 h apart, part of the differences may be related to time changes. A neutrally stratified mixed layer developed over both sur-

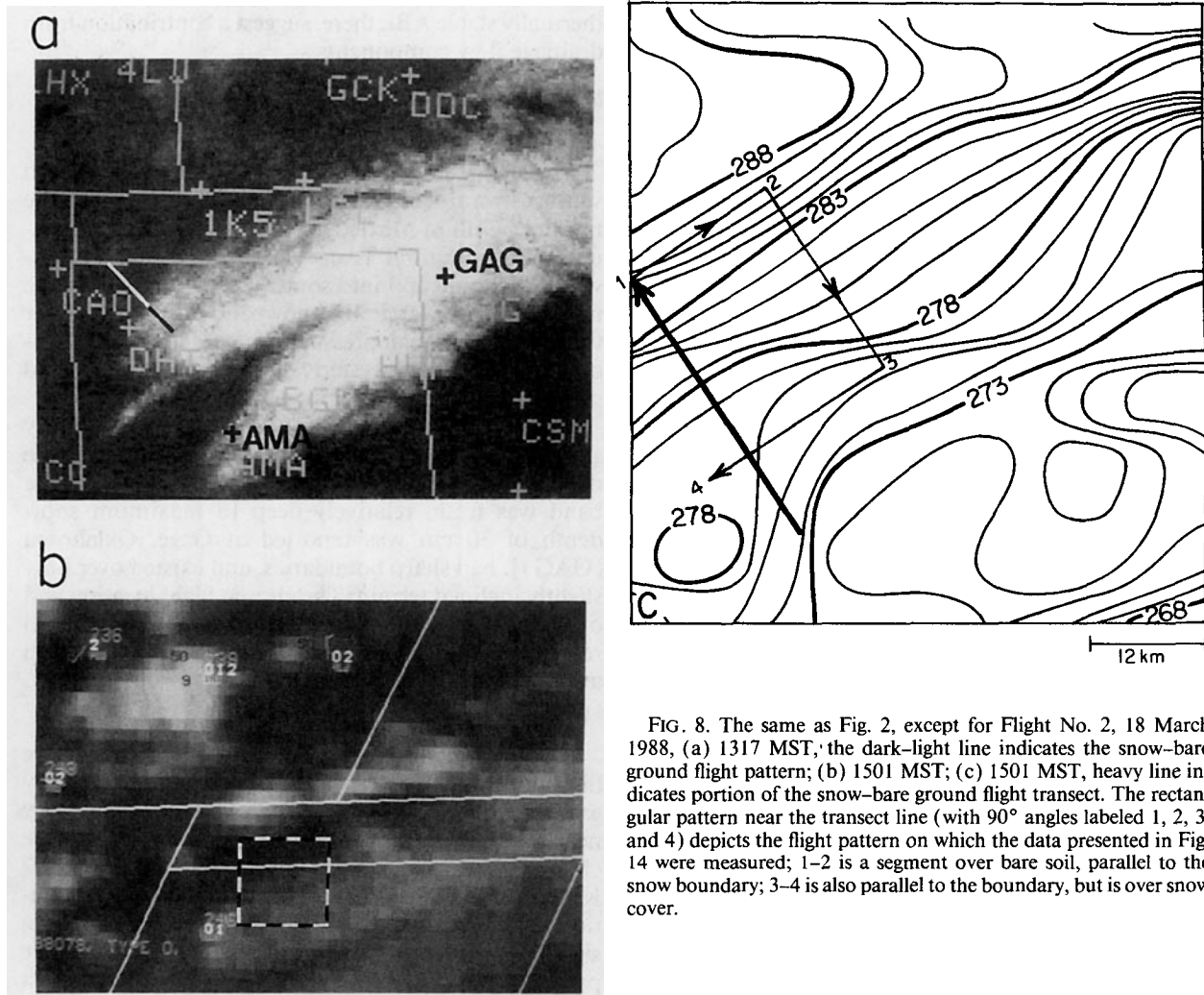


FIG. 8. The same as Fig. 2, except for Flight No. 2, 18 March 1988, (a) 1317 MST, the dark-light line indicates the snow-bare ground flight pattern; (b) 1501 MST; (c) 1501 MST, heavy line indicates portion of the snow-bare ground flight transect. The rectangular pattern near the transect line (with  $90^\circ$  angles labeled 1, 2, 3, and 4) depicts the flight pattern on which the data presented in Fig. 14 were measured; 1-2 is a segment over bare soil, parallel to the snow boundary; 3-4 is also parallel to the boundary, but is over snow cover.

faces; the  $\theta$  profiles in Figs. 11a,b indicating an ABL depth of at least 1800 m over the snow-free region and only about 500 m over the snow. The profiles show that, over the snow, the lowest several hundred meters of the atmosphere were about 7 K cooler than the comparable low-level air over the bare region, suggesting a significant potential for a snow-breeze flow. Over both regions the flow was generally north-northwesterly (Figs. 11c,d). In the near surface layer the flow was  $5\text{--}8\text{ m s}^{-1}$  over the bare region, tending to westerly; the wind speed was only  $1\text{--}3\text{ m s}^{-1}$  over the snow (Figs. 11e-f). Thus, the interaction of thermally induced flow and the opposing synoptic flow is indicated.

Only low-altitude measurements (along transects) were carried out in Flight No. 2; results are presented in the following. The change in the sensible heat flux,  $H_s$ , along the 90-m transect outlined in Fig. 12a was from a peak of about  $200\text{ W m}^{-2}$  over the snow-free area to the lowest value of  $\sim 25\text{ W m}^{-2}$  over the snow-

covered area, with much of that change occurring within a 5-km zone. Corresponding variations in  $\theta$  of 5 K occur along the transect (Fig. 12b). The winds over the bare ground region reflected the background flow of  $4\text{--}8\text{ m s}^{-1}$  from the north-northwest (Figs. 12c,d). This flow would be expected to oppose a mesoscale circulation induced by the surface contrast, as indeed seems to occur, with the flow on the snow side of the boundary generally south-southeasterly at about  $1\text{ m s}^{-1}$ . Since the background flow was from a direction opposing the snow breeze, a frontal-like structure in the near-surface  $\theta$  field near the snow boundary was generated. In calm conditions, it would be expected that the snow breeze could extend to a considerable distance over the bare ground (i.e., analogous to a sea breeze).

In a second flight along the same transect about an hour later, the  $H_s$  and the  $\theta$  changes across the snow-bare ground boundary are very noticeable (Figs. 13a,b). A more developed snow breeze (Figs. 13c,d), as com-

pared to the earlier observations, is evident. The change in the wind direction near the boundary is very sharp, with the snow breeze there reaching about  $4 \text{ m s}^{-1}$  in intensity.

A 90-m altitude transect for the pattern indicated by the thin arrowed line in Fig. 8c was also performed. The data from this leg (Fig. 14) established the existence of the observed atmospheric contrasts through some distance parallel to the snow-bare ground boundary. The surface temperature,  $T_s$ , and the  $\theta$  values along the bare ground section (indicated as 1-2 in Fig. 8c) are very noticeably higher than those related to the snow-covered section (3-4 in Fig. 8c). The snow breeze is evident through the  $180^\circ$  change in wind direction from the bare ground to the snow-covered area (although due to the strong background flow it is noticeable only within a shallow layer of  $\sim 100 \text{ m}$ ).

Of the 9 SSBLIM flights, the data from this flight produced the best evidence in support of the snow-breeze hypothesis. Although the snow region was somewhat patchy, the moderate opposing (relative to the snow breeze) background flow actually enhanced the observed atmospheric gradients.

d. Flight No. 3 (Texas Panhandle, 19 March 1988)

1) SITUATION

Since the results from Flight No. 2 were strongly supportive for the existence of a noticeable snow breeze, Flight No. 3 was made the following day (19 March 1988) over the same snowband. A surface pressure synoptic map is given in Fig. 15. The shape and extent of the snow was modified due to melting (Fig. 16a).

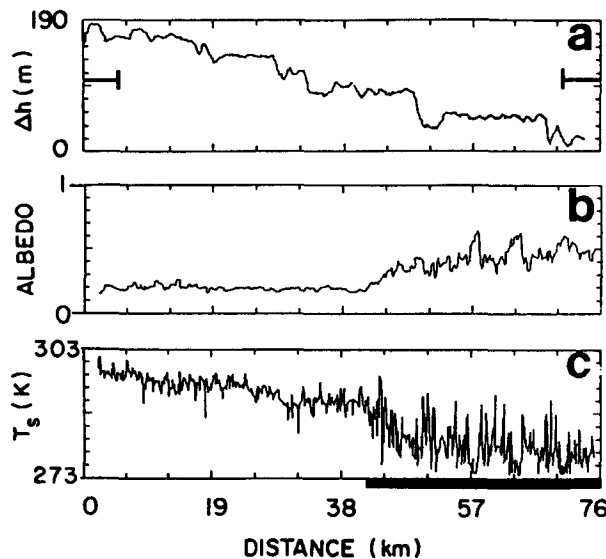


FIG. 9. The same as Fig. 3 except for Flight No. 2 and based on flight altitude data measured at 1413:50-1428:43 CST. The dark line indicates snow cover. See Figs. 8a,b for flight transect.

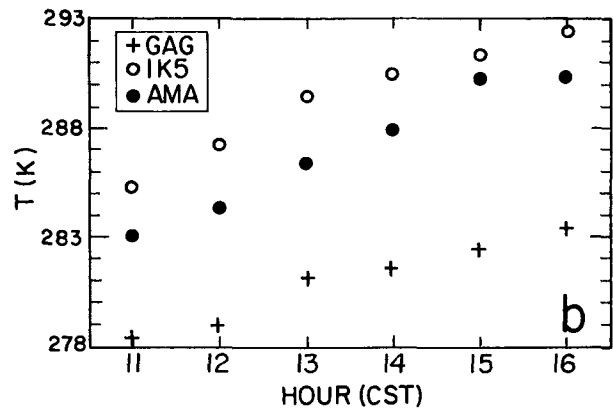


FIG. 10. Daytime variation of shelter temperature at the stations: GAG (Gage, Oklahoma: snow covered); AMA (Amarillo, Texas: snow-bare ground boundary); and 1K5 (Oklahoma: snow free), on 18 March 1988.

A new flight location, shown in Fig. 16a, was chosen. The most significant synoptic changes from the previous day consisted of a stronger background flow (westerly flow that intensified gradually during the day, reaching  $\sim 13 \text{ m s}^{-1}$  at 100 m during the flight) with higher air temperatures. Despite the strong synoptic flow, several observed features associated with a snow breeze were still found.

2) MEASUREMENTS

The 1410 MST (1510 CST) satellite-derived surface temperature gradients for this flight were, again, substantial (Fig. 16b). Figure 16c shows a broad transition zone across the snow-bare ground boundary, with a surface temperature change of 14 K in 26 km ( $\sim 0.54 \text{ K km}^{-1}$ ). This is similar to the surface temperature gradient observed by the aircraft (Fig. 17; see Fig. 16a for flight transect location and orientation). The surface temperature and albedo measurements indicate that the snow-bare ground boundary was a rather broad transition zone, with satellite imagery throughout the day showing a progressive melting and shrinkage of the snow area. The overall surface temperature change along the flight transects was large, from about 272 K to about 299 K over bare ground.

The background synoptic flow was westerly (at about a  $45^\circ$  angle to the flight pattern) at about  $13 \text{ m s}^{-1}$ , suggesting that any snow breeze would be heavily suppressed. Nevertheless, the contrast in thermal stratification implies the potential for the development of a snow breeze in similar environmental conditions but in the absence of any significant synoptic flow (see section 3). The  $H_s$  values over the bare ground were noticeably higher than those computed over the snow-covered area (except for the 450-m altitude leg)—see Fig. 18. The  $H_s$  values over bare ground reached peak values of  $\sim 150 \text{ W m}^{-2}$ , compared with minimum val-



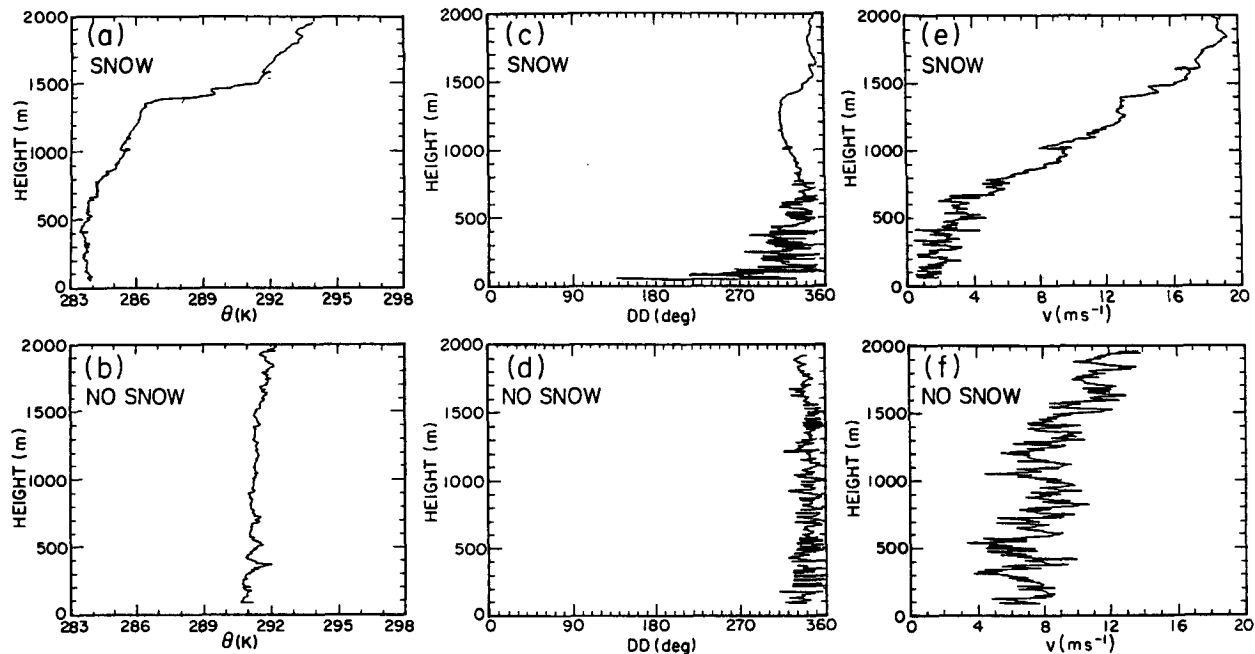


FIG. 11. Vertical profiles of several variables from Flight No. 2 at the locations indicated by Fig. 9a. Snow measurements were made from 1355:40–1413:17 CST; bare ground measurements were made from 1536:23–1547:00 CST; (a–b) potential temperature; (c–d) wind direction,  $DD$ ; and (e–f) wind speed,  $V$ .

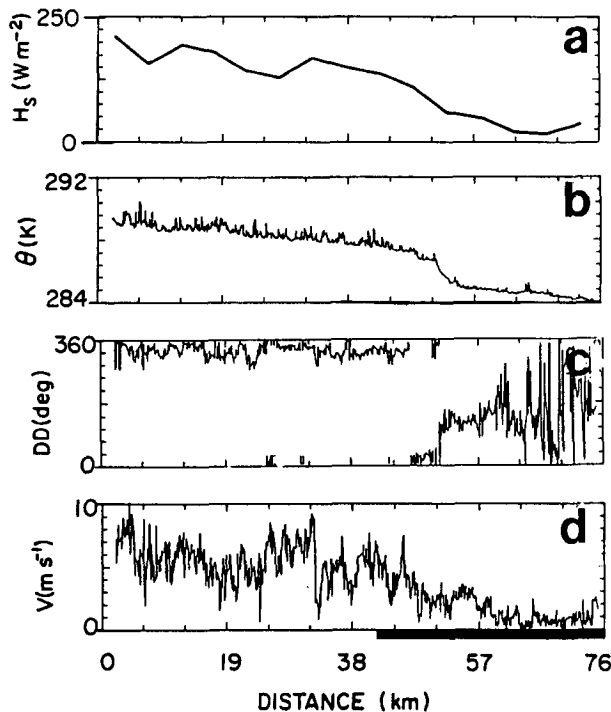


FIG. 12. Variables measured along the 90-m altitude transect in Flight No. 2 (from 1413:50–1428:43). The dark line indicates the snow-covered portion of the transect. (a) Sensible heat flux,  $H_s$ ; (b) potential temperature,  $\theta$ ; (c) wind direction,  $DD$ ; and (d) wind speed,  $V$ .

ues  $\sim -25 \text{ W m}^{-2}$  over the snow-covered area. These patterns of change in  $H_s$  are consistent with the gradual increase in air temperature of about 3–5 K at all altitudes, as the aircraft proceeded from the snow toward the bare ground (Fig. 19).

For this flight, with a relatively strong synoptic flow, the only observable snow-breeze effect relates to the wind field near the snow–bare ground boundary. Over the snow, winds were slightly stronger in magnitude and more southerly in direction than elsewhere (not shown). Although this case was far from ideal in clearly identifying a snow breeze, its use lies in demonstrating the ability of snow to modify the ABL characteristics, even in conditions of relatively strong wind.

#### e. Other flights

As mentioned previously, six additional flights were carried out during the SSBLIM. However, less distinctive features related to snow effects were observed in these flights. Although results from these flights are not presented, it is worth noting the reasons for the reduced snow effects: 1) *strong winds*—preflight underestimation of the wind speed was related to an intensification of the surface wind around midday (usually following flight takeoff), or due to a lack of meteorological reports in the measurements area. In these cases the surface temperatures over the snow were noticeably lower than those of the adjacent bare ground area, and differences in the ABL temperature were measured (e.g., 8 March

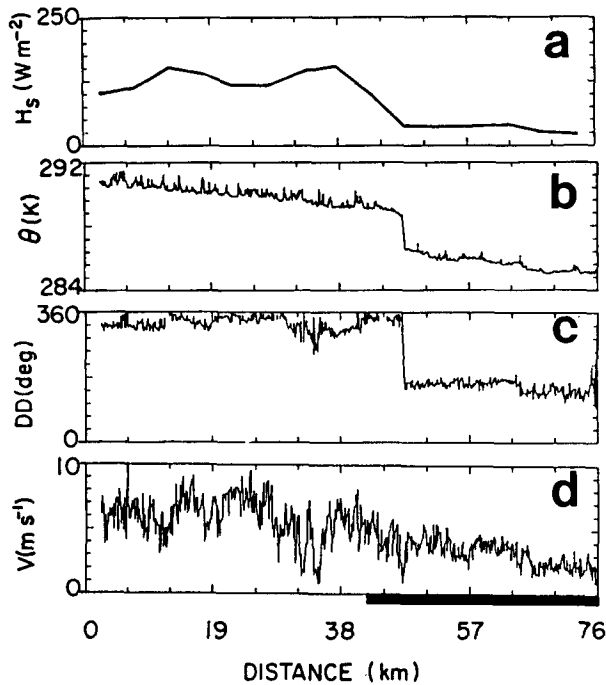


FIG. 13. The same as Fig. 12, except for 1521:30–1536:23 CST.

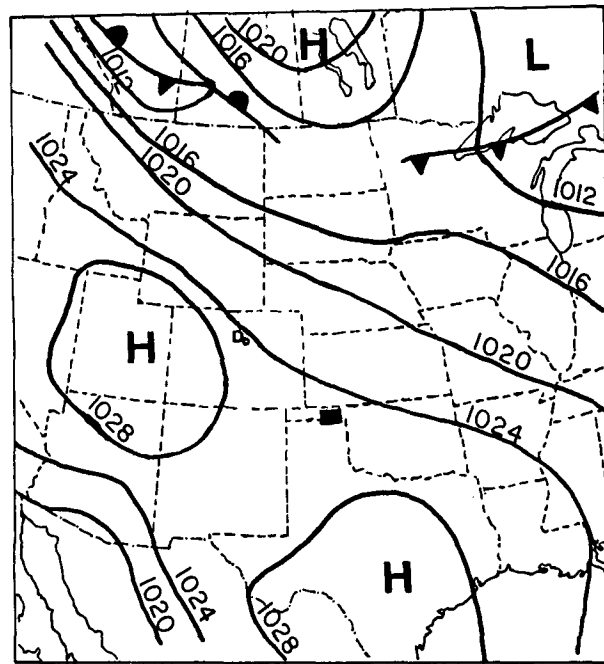


FIG. 15. As Fig. 1, except for 19 March 1988.

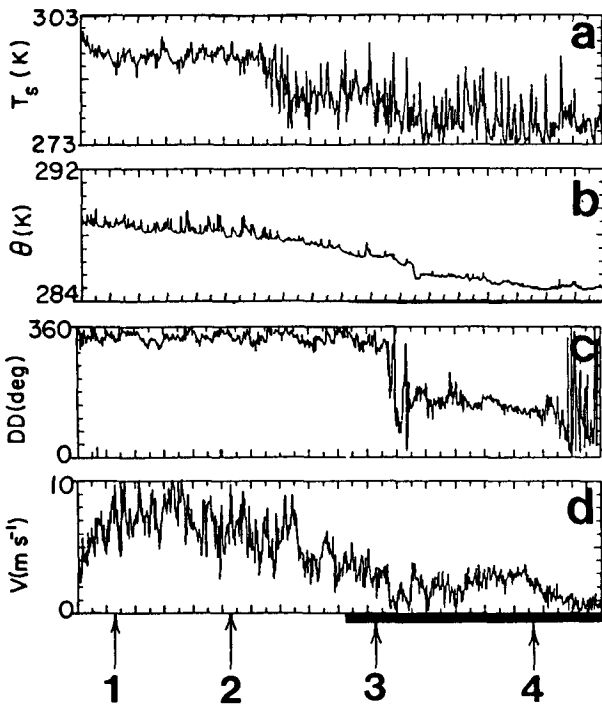


FIG. 14. Measured (a) surface temperature,  $T_s$ ; (b) potential temperature,  $\theta$ ; (c) wind direction,  $DD$ ; and (d) wind speed,  $V$ , along the 90-m flight; data measured from 1435:00–1453:00 CST (Flight No. 2). The arrows indicate the locations of the four  $90^\circ$  turns shown in the schematic flight path superimposed on Fig. 8c. The dark line indicates snow-covered portion of transect. One tick mark interval along the abscissa is about 2.4 km.

1988, south of Pueblo, Colorado); 2) *fast snow melting*—situations involved with a small amount of snowfall over relatively warm ground, which were associated with daytime warming during the flight hours, led to an extremely rapid melting. On 5 March 1988, for example, over an area of horizontal scale of greater than 100 km in southeast Colorado, uniform snow-cover was indicated on the late morning GOES satellite visible imagery. However, by noon (local time) only isolated small patches of snow were observed from the aircraft; and 3) *bare ground patches* in the snow cover due to partial snow melt (e.g., 17 February, the Front Range of Colorado). Some thermal stabilization and a reduction in the ABL temperature over the snow area were noticed when conditions in 2) and 3) occurred. These features are attributed to the partial snow cover, as well as to wet ground due to snow melting.

### 3. Scaling considerations based on observations

#### a. Surface temperature

The difference in the surface temperature,  $\Delta T$ , between land and water surfaces was used in early numerical model studies as a forcing function in sea-breeze simulations. Thus, with sea-surface temperatures of  $\sim 298$  K and midday surface temperatures greater than 310 K over dry ground in midlatitudes during the summer (e.g., Pielke and Cotton 1977; and Segal et al. 1989),  $\Delta T > 12$  K. The related satellite and aircraft-derived  $\Delta T$  during the SSBLIM project presented previously (with a snow surface replacing

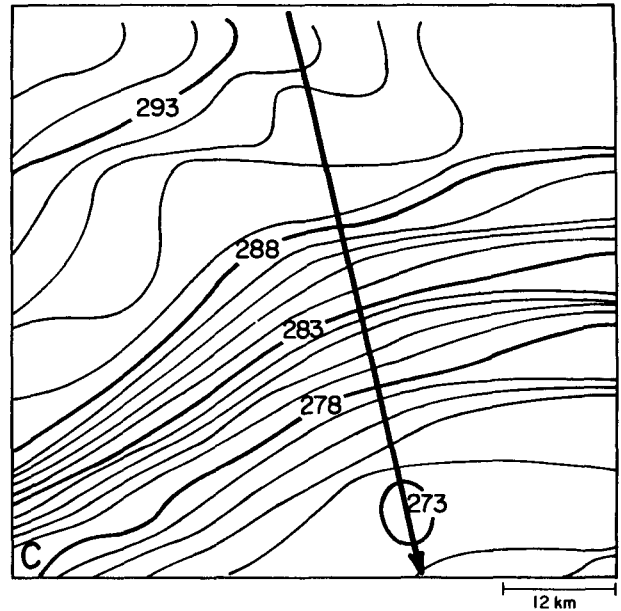
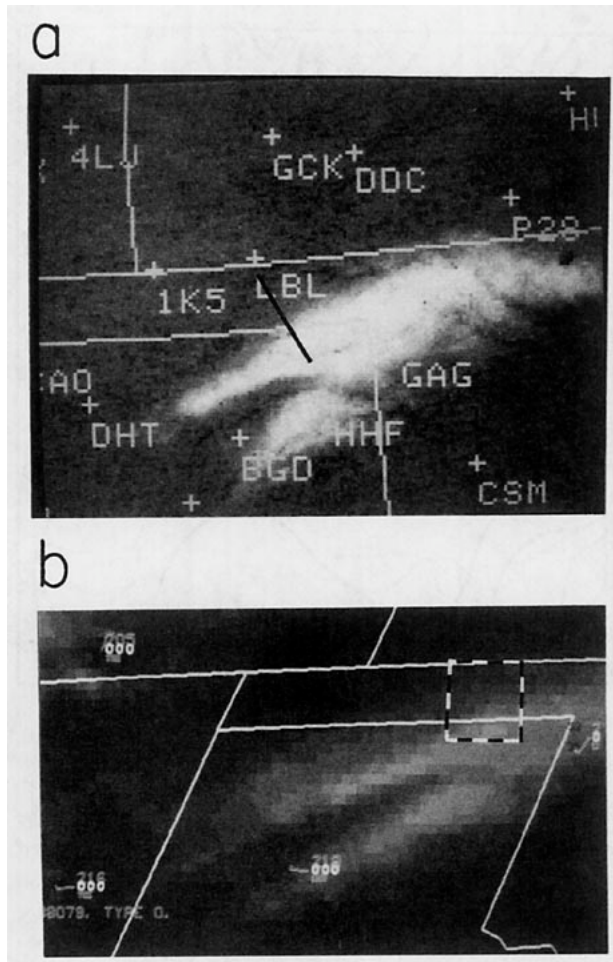


FIG. 16. The same as Fig. 2 except for Flight No. 3 19 March 1988, (a) 1647 CST, the dark line indicates the flight pattern; (b) 1345 CST; and (c) 1345 MST, the dark line indicates the flight pattern.

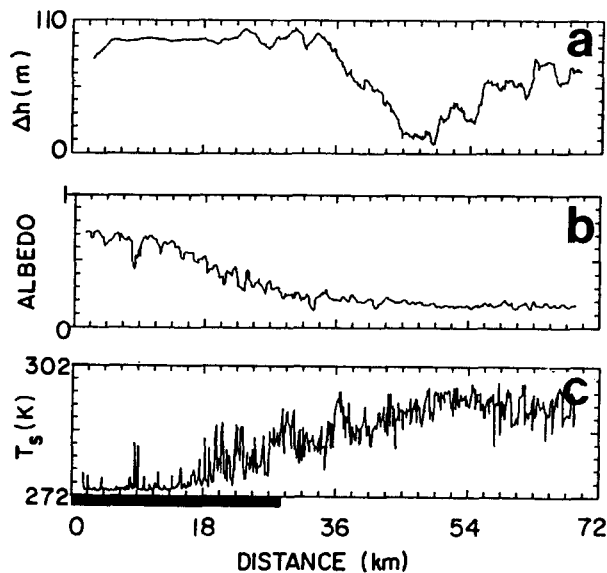


FIG. 17. The same as in Fig. 3 except for Flight No. 3. See Fig. 16a for flight transect.

the water surface) reached values of  $\sim 20$  K (in flights No. 2 and No. 3). Following Biggs and Graves (1962) and Walsh (1974), the  $\Delta T$  values can be used to estimate the speed of the sea-breeze flow at the surface,  $V_{SB}$ , in the absence of synoptic flow namely using  $V_{SB} \approx (\beta \Delta T)^{1/2}$  where  $\beta \approx 1.5$ .

Use of such relations for estimating snow-breeze intensity should be made with caution, however, since overestimation is likely. To see this, consider that the constraint on the snow-surface temperature of less than 273 K is likely to involve the generation of a shallow surface-temperature inversion without any substantial thermal-forcing of the snow breeze. The intensity of the snow breeze can be related to the difference in time-integrated surface sensible heat flux,  $\Delta \hat{H}_s$ , between the snow and snow-free locations, where:

$$\Delta \hat{H}_s \approx \rho c_p [C_D U (T_a - T_s)_{|snow\ free} - C_D U (T_a - T_{sn})_{|snow}] \tau \quad (1)$$

with  $C_D$  as the drag coefficient;  $U$  the surface wind speed;  $T_a$  the air temperature at a reference level above

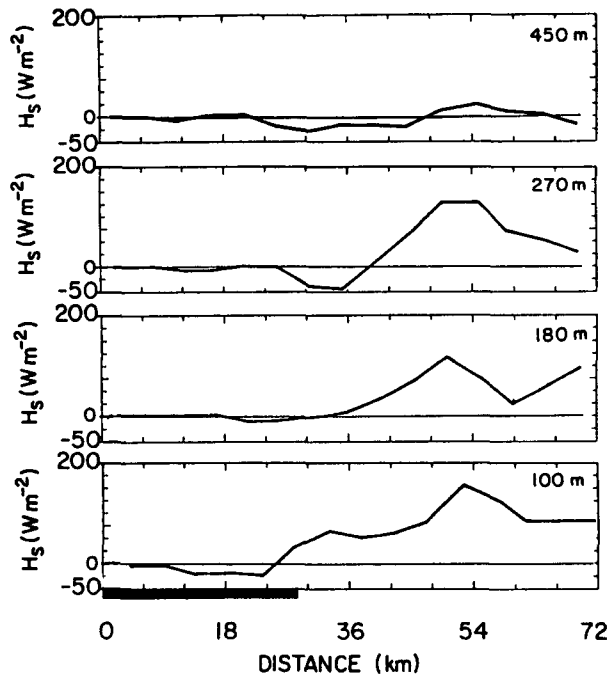


FIG. 18. Sensible heat fluxes measured at various altitudes, Flight No. 3: 100-m data measured from 1314:00–1327:05 CST; 180-m data measured from 1329:04–1342:10; 270-m data measured from 1345:08–1359:15; 450-m data measured from 1401:25–1414:35 CST. The dark line indicates the snow-covered portion of transect.

the surface;  $T_s$  the snow-free surface temperature;  $T_{sn}$  the snow surface temperature;  $\rho$  the air density;  $c_p$  the specific heat of air at constant pressure; and  $\tau$  the time scale for the duration of the circulation.

The second term on the rhs of Eq. (1) is much smaller than the first and has, in general, no influence on the scaling of the snow-breeze intensity. Thus, increasing  $T_{sn}$  toward  $T_a$ , or even somewhat above  $T_a$  (and therefore, reducing  $\Delta T$ ), over the snow has little effect on  $\Delta H_s$ . (Over sea surfaces, the seasonal values of  $T_a$  and  $T_s$  are, in most cases, closer in value). Thus, the values of  $\Delta T$  reflecting the snow–snow-free surface temperature difference will overestimate it when using the empirical relations suggested for sea breezes (although qualitatively indicating the potential intensity of snow breezes).

*b. Surface pressure gradient*

A simplified scale analysis similar to that adopted in Segal et al. (1989) is presented here, in order to aid in the interpretation of the observed features presented in the previous subsections.

Adopting the hydrostatic relation, the surface pressure difference,  $\Delta p_0$ , between a point in the middle of the snow-covered domain and one in the bare ground region is given by:

$$\Delta p_0 = p_z \left[ \exp \left( \int_0^z \frac{g}{RT_s} dz \right) - \exp \left( \int_0^z \frac{g}{RT_{bg}} dz \right) \right] \quad (2)$$

where:

$p_z \approx$  the pressure at level  $z$  over the measurement area, in the range 800–850 mb

$z =$  the height above the surface at which no temperature difference between the bare ground and the snow area is observed

$g =$  gravitational acceleration

$T_s, T_{bg} =$  air temperatures above the snow and bare ground, respectively ( $\Delta T = T_{bg} - T_s$ )

$R =$  the gas constant.

Flight results suggest that no significant  $\Delta T$  values exists above  $z \sim 1000$  m, although nonzero  $\Delta T$  values above  $z \sim 500$  m may not be associated with the surface thermal forcing. Thus, using typical values,  $\Delta T_{z=0} \approx 5.5$  K; and  $\Delta T_{z=500 \text{ m}} \approx 0$  and linear reduction of  $\Delta T$  with height yields for a dry atmosphere,  $\Delta p_0 \approx 0.5$  mb. For individual flights, using the observed profiles of  $\Delta T$ , values of  $\Delta p_0$  ranged between 0.3 and 1.4 mb. Table 1 (a condensed version of that in Segal et al. 1989) provides data on horizontal temperature differences obtained in observational studies and model simulations of sea-breeze flows. The table gives selected values of  $\Delta T$  and  $\Delta p_0$  across a 20-km line centered (a) on the coastline; (b) at the sea-breeze front, showing that  $\Delta T$  at several hundred meters may reach several degrees Kelvin across both the coastline and across the

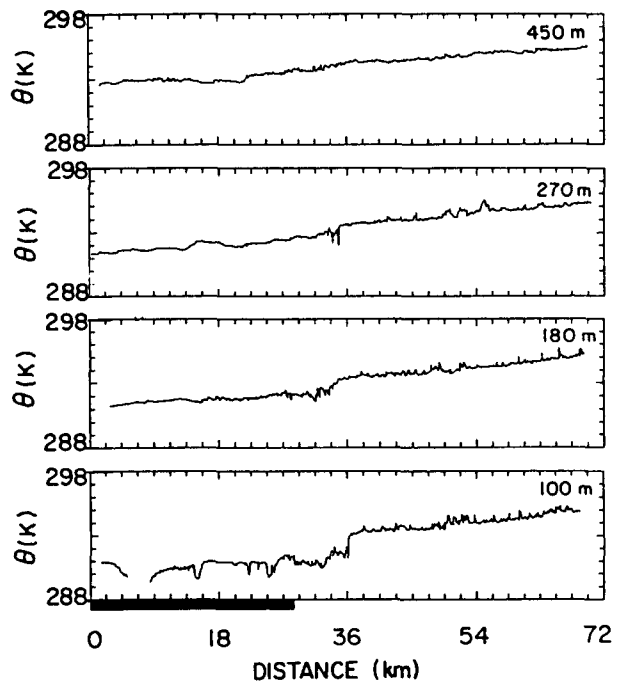


FIG. 19. Potential temperature,  $\theta$ , for the transect altitudes indicated in Fig. 18.

TABLE 1. Summary of Table 1 of Segal et al. (1989) showing horizontal temperature ( $\Delta T$ ) and surface pressure ( $\Delta p_0$ ) differences along a 20-km line centered on either the coastline or the inland sea-breeze front. Here  $z_1$  is a near-surface level,  $z_2 = 150$  m and  $z_3 = 440$  m; the synoptic wind is designated as light (*L*) or moderate (*M*).

Location	Data source	$\Delta T(K)$			$\Delta p_0$ (mb)	Synoptic wind
		$z_1$	$z_2$	$z_3$		
Coastline	Observations	3.5	3	1	0.5	<i>L</i>
	Model	~5	~2	~0.5	~0.2	<i>L</i>
Inland	Observations	0.7	~2	0-2	~0.5	<i>L-M</i> (onshore)
	Model	0-2	~2	~2	~0.5	<i>L-M</i> (onshore)

sea-breeze front deep inland and be associated with surface pressure differences of approximately 0.5 mb. The temperature changes observed along some of the transects in the current study, and the implied values of  $\Delta p_0$  based on Eq. (2), are comparable to those indicated in some of the sea-breeze cases.

#### 4. Discussion

Observations evaluating the potential impact of snow-covered areas on the generated snow breezes have been described. Surface observations can provide potentially useful information although, typically, the random boundaries of snow-bare ground areas and the relatively low-intensity solar radiation in the winter months make it difficult to identify snow-breeze flows with existing surface meteorological networks. However, these networks are on many occasions capable of quantifying the surface thermal difference between snow-covered areas and snow-free areas, and so provide a broad indication of the potential for the generation of snow breezes. Satellite IR imagery (in clear sky conditions) can be used for further quantification of the surface temperature contrast.

In order to avoid the limitations indicated above for studying snow breezes through surface observations, and in order to enhance the insight into its vertical structure, aircraft measurements were carried out. Unfortunately during the project period, the available opportunities were not ideal for the optimum identification of snow breezes. Although well-defined snow-bare ground boundaries associated with significant thermal contrasts were observed, they were associated with relatively strong winds. Even under these conditions, snow-breeze flows were identified in two cases, while in all others (with pronounced thermal contrasts) strong synoptic flow generally masked the presence of any snow breeze. Over a larger region, well-defined boundaries between snow-bare ground areas, under clear sky and light synoptic flow conditions, are common at various locations during the snow season. It is suggested, based on the thermal contrasts observed in this study, that noticeable snow breezes are likely to occur in these regions. It is likely that snow events in the winter southern latitudes, or at midlatitudes in the

early and late winter season, provide conditions giving the most pronounced snow breezes.

*Acknowledgments.* The study was supported by NSF Grants ATM-8616662 and ATM-8915265 and EPRI Contract RP-1630-53. Portions of the study formed the basis for the Master of Science thesis of the second author. The SSBLIM project was carried out using the NCAR King Air Aircraft operated by the NCAR Aviation Division. The BAO meteorological data was obtained from NOAA/ERL at Boulder. GOES satellite imagery and other real-time meteorological data in support of the SSBLIM was obtained by the PROFESSERS at the Cooperative Institute for Research of the Atmosphere (CIRA), and at the NOAA/NESDIS/RAMM Branch Data Utilization Center (VDUC), CSU. We would like to thank A. Schanot and G. Summer and their staff for the management of the aircraft measurements, and D. Wolfe for his help relating to access to the BAO data. G. Kallos, J. Purdom, J. Weaver, Z. Ye, and R. Zehr provided useful help during the SSBLIM operational phase. The authors would also like to thank B. Critchfield and D. McDonald for preparing the manuscript and J. Sorbie for drafting of the figures.

#### REFERENCES

- Biggs, W. G., and M. E. Graves, 1962: A lake breeze index. *J. Appl. Meteor.*, **1**, 474-480.
- Bluestein, H. B., 1982: A wintertime mesoscale cold front in the southern plains. *Bull. Amer. Meteor. Soc.*, **63**, 178-185.
- Cramer, J., 1988: Observational evaluation of snow-cover effects on the generation and modification of mesoscale circulations. Paper #439, Department of Atmospheric Science, 143 pp.
- Garratt, J. R., and B. F. Ryan, 1988: The structure of the stably stratified internal boundary layer in offshore flow over sea. *Bound.-Layer Meteor.*, **47**, 17-40.
- Johnson, R. H., G. S. Young, J. J. Toth and R. M. Zehr, 1984: Mesoscale weather effects of variable snow cover over northeast Colorado. *Mon. Wea. Rev.*, **112**, 1141-1152.
- Lenschow, D. H., and P. Spyers-Duran, 1987: Measurement techniques: Air motion sensing. *NCAR RAF Bulletin No. 23*, NCAR, 47 pp.
- Mahrer, Y., and M. Segal, 1979: Simulation of advective Sharav conditions in central Israel. *Isr. J. Earth Sci.*, **28**, 103-106.
- Miller, E. R., and R. B. Friesen, 1987: Standard output data products from the NCAR Research Aviation Facility. *NCAR RAF Bulletin No. 9*, NCAR, 70 pp.
- Pielke, R. A., and W. R. Cotton, 1977: A mesoscale analysis over south Florida for high rainfall events. *Mon. Wea. Rev.*, **105**, 343-362.
- Schlatter, T. W., V. D. Barker and J. F. Henz, 1983: Profiling Colorado's Christmas Eve blizzard. *Weatherwise*, **36**, 60-66.
- Segal, M., W. E. Schreiber, G. Kallos, J. R. Garratt, A. Rodi, J. Weaver and R. A. Pielke, 1989: The impact of crop areas in northeast Colorado on midsummer mesoscale thermal circulations. *Mon. Wea. Rev.*, **112**, 809-825.
- , J. R. Garratt, R. A. Pielke and Z. Ye, 1991: Scaling and numerical model evaluation of snow-cover effects on the generation and modification of daytime mesoscale circulations. *J. Atmos. Sci.* (in press).
- Walsh, J. E., 1974: Sea-breeze theory and application. *J. Atmos. Sci.*, **31**, 2012-2026.
- Wash, C. H., D. A. Edman and J. Zapotocny, 1981: GOES observation of a rapidly melting snow-band. *Mon. Wea. Rev.*, **109**, 1353-1356.